

Investigation of structural, thermal and dielectric properties of PVC/modified magnetic nanoparticle composites

Abdulahman TUKUR¹ , Mustafa Ersin PEKDEMİR^{1*} , Mehmet ÇOŞKUN¹ 

¹ Fırat University, Chemistry Departmenty, 23119, Elazığ/ TURKEY

Abstract

Three different composites (5, 10, and 20 wt. %) were prepared using purified PVC and POH-g-N₃PTMS-g-Fe₃O₄. Firstly, 3-azidopropyltrimethoxysilane was synthesized under reflux from 3-chlorotrimethoxysilane and sodium azide. Then, magnetic nanoparticle was bonded with the silane group of 3-azidopropyltrimethoxysilane. After that the 3-azidopropyltrimethoxysilane bearing magnetic nanoparticle undergo click reaction with propargyl alcohol, and then the composites were prepared. Some characterization, including FT-IR spectroscopy, SEM, Differential scanning calorimetry (DSC), vibrating sample magnetometer (VSM), and EDX images was performed to the composites. The DSC measurements showed that the click reaction of the 3-azidopropyltrimethoxysilane graft magnetic nanoparticles (N₃PTMS-g-Fe₃O₄) reduced the glass transition temperature (T_g). Click reaction reduced the thermal stability of N₃PTMS-g-Fe₃O₄. The thermal stabilities of the composites increased by increasing the compositional rate. It was found that the 10% PVC /POH-g-N₃PTMS-g-Fe₃O₄ reached saturation magnetization (M_s) at 5.12 emu/g. The dielectric constant (ϵ') and dielectric loss (ϵ'') of POH-g-N₃PTMS-g-Fe₃O₄ rapidly decreased with increasing applied frequency and then remain more or less constant. Also, the AC conductivity (σ_{ac}) increased sharply with increasing the applied frequency. While the ϵ' decreased slightly for the composites by increasing the applied frequency and the σ_{ac} increase dramatically with an increase in applied frequency at room temperature.

Article info

History:

Received:07.04.2020

Accepted:04.06.2020

Keywords:

PVC,
Fe₃O₄ nanoparticles,
Click reaction,
Composite,
Dielectric.

1. Introduction

The unique electrical, thermal, optical, electronic, and mechanical characteristics properties of metal nanoparticles and nanocomposites make them the subject of extensive researches. Polymers, as ideal host matrices, are good candidates for composite materials [1]. Materials having magnetic properties are of great interest to many possible applications. Amid the number of magnetic nanomaterials, Fe₃O₄ nanoparticles attracted far attention owed to their unique properties [2]. Recently, inorganic-polymer composite has been studied deeply due to their specific use and properties [3], e.g., magnetite/polymer nanocomposite is one of the attractive nanocomposites [4]. Due to its wide applications, poly(vinyl chloride) (PVC) is picked as the host polymer matrix. PVC is a polymer that has lots of characteristics suitable for industrial applications, such as good mechanical properties, good processability, fire retardancy, and good resistance to acidic and basic environments.

Additionally, PVC has a desirable properties, including low cost of production, biocompatibility, and chemical stability [5]. PVC thermal and mechanical properties can be improved by additives addition such as clay, wood fibers and flour, and calcium carbonate [5]. The electrical properties of PVC can be enhanced through incorporating zinc oxide nanorods [6], conjugated polymers (such as polyaniline and polypyrrole) [7], SiO₂ nanoparticle [8], and carbon black [9] embeded in the PVC matrix. The simultaneous presence of Fe₃O₄ nanoparticles, and graphene serve as a nanofiller in the PVC matrix which increases the young's modulus, tensile strength, and conductivity compared to that of pure PVC [10]. These improvements are linked to the synergistic effect of the host polymer and nanometer dimensional dispersion of inorganic nanoparticles. Furthermore, thermal stability studies and dielectric properties of various important polymers and their composites have been studied. Magnetic nanoparticles bonded to PVC with the help of click reaction showed an increase in thermal stability and dielectric constant compared to pure PVC. The saturation magnetization

*Corresponding author. Email address: ersinpkdmr58@gmail.com

value revealed that the product is a superparamagnetic [11]. Magnetic nanocomposite prepared by Fe₃O₄ nanoparticles and polystyrene can be used for microelectromechanical systems, since it shows good electrical conductivity [3]. The influence of magnetic nanoparticles was studied for chitin/cashew biopolymer composites, and the results revealed that an increase in thermal stability and the dielectric properties was improved due to the interaction with Fe₃O₄ nanoparticles [12]. Likewise, Fe₃O₄ nanoparticles/polymer composite was studied for polyvinyl butyral/magnetite (PVB/Fe₃O₄) and polymethylmethacrylate/magnetite (PMMA/Fe₃O₄) composites [13], pectin-magnetite nanocomposite [14], superparamagnetic iron oxide nanoparticles, graphene oxide, chitosan, and poly(vinyl alcohol) biocompatible polymers [15].

In this study, the 3-chloropropyltrimethoxysilane was reacted with sodium azide in the presence of tetraethylammonium bromide to form 3-azidopropyltrimethoxysilane. This is bounded to Fe₃O₄ nanoparticles. The modified magnetic nanoparticle formed undergoes click reaction with propargyl alcohol to form Fe₃O₄ nanoparticles bearing 1,2,3-triazole ring and then, three composites of PVC were prepared by embedding the modified Fe₃O₄ nanoparticles with various concentrations. FT-IR spectroscopy and SEM/EDX were used for structural characterization. DSC and TGA techniques were used for glass transition temperature and thermal stability of the composites. The magnetic property of 10% composite was investigated using vibrating sample magnetometry (VSM). And lastly, dielectric and AC conductivity properties of the modified Fe₃O₄ nanoparticles and composites were studied.

2. Materials and Methods

2.1. Apparatus

T Perkin-Elmer Spectrum one FT-IR spectrometer was used to record Infrared spectra. Morphology studies were performed with the Zeis EVO MA10 scanning electron microscope (SEM). Calorimetric measurements were accomplished using PerkinElmer instruments Sapphire DSC at a heating rate of 20 °C/min under N₂ flow. Thermal stability were recorded using PerkinElmer instruments Pyris Diamond TGA under N₂ flow at a heating rate of 10 °C/min. Dielectric measurements were carried out using QuadTech 7600 precision LCR meter. Magnetic properties was investigated using Quantum Design PPMS-9T.

2.2. Synthesis of 3-azidopropyltrimethoxysilane (N₃PTMS)

NaN₃ (2.14 g, 33.2 mmol), 3-chloropropyltrimethoxysilane (CITMS) (3.30 g, 16.6 mmol), and tetraethylammonium bromide (TEABr) (0.84 g, 4 mmol) were passed into a single neck round bottom flask stocked with reflux condenser containing 50 mL acetonitrile, under argon atmosphere. The reaction continued under reflux for 18 h. The solvent was evaporated after completion, the crude like mixture acquired was diluted in dry hexane and filtered. The solvent was evaporated and the colorless liquid formed is 3-azidopropyltrimethoxysilane [16].

2.3. Bonding of magnetic nanoparticle (Fe₃O₄) to 3-azidopropyltrimethoxysilane (N₃PTMS)

Fe₃O₄ nanoparticles (2.00 g) was homogenized for 30 min in 75 mL absolute ethanol. N₃PTMS (2.00 g) was added and Argon was injected for about 15 min, and the process continued at ambient temperature for 6 h, then under reflux for 48 h. Fe₃O₄-g-N₃PTMS was separated magnetically, then washed with alcohol, and dried at room temperature followed by vacuum for 24 h at 50 °C.

2.4. Click reaction of N₃PTMS-g-Fe₃O₄ and propargyl alcohol (POH)

In a flask, N₃PTMS-g-Fe₃O₄ (1.00 g) was homogenized for 30 min in 15 mL dimethylformamide (DMF). Then propargyl alcohol (POH) (1.33 g) was added to the solution. After that Cu(I)Br 0.07 g (0.48 mmol) and 5,5'-dimethyl-2,2'-dipyridyl 0.22 g (0.48 mmol) were dissolved in 5 mL DMF in a beaker and poured to the previous solution. Argon was passed for 15 min and continued at 30 °C for 24 h. The product was washed under a magnet with dichloromethane and dried at room temperature for 24 h followed by vacuum at 50 °C for 24 h.

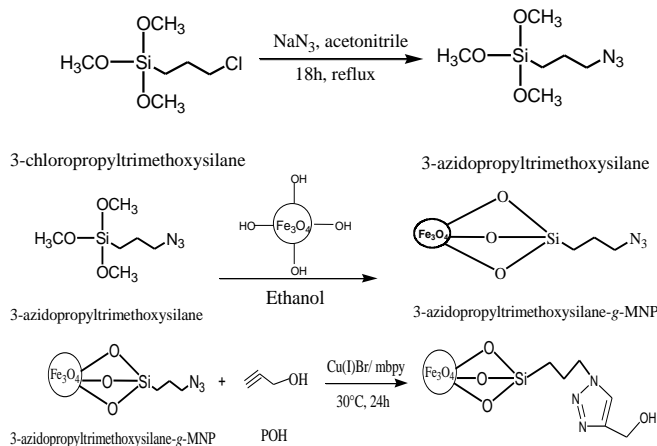
2.5. Preparation of composite of PVC with POH-g-N₃PTMS-g-Fe₃O₄

Firstly, 10 mL tetrahydrofuran (THF) was used to dissolve PVC (0.50 g). 5% (0.025 g) POH-g-N₃PTMS-g-Fe₃O₄ was added to the mixture and sonicated for 45 min. The solution was precipitated in ethanol, filtered, dried at room temperature, and then vacuum for 24 h at 45 °C. The procedure abovementioned was used to prepare 10% (0.05 g) and 20% (0.10 g) composites.

3. Results and Discussion

3.1. FTIR and SEM characterization

3-azidopropyltrimethoxysilane was formed by a nucleophilic substitution reaction of 3-chloropropyltrimethoxy-silane and sodium azide (Scheme 1).



Scheme 1. Reaction pathways in the synthesis of POH-g-N₃PTMS-g-Fe₃O₄

The FT-IR spectrum of 3-azidopropyltrimethoxysilane (Figure 1a) shows an absorption band at 2101 cm⁻¹ which is distinctive and characteristic stretching vibration for -N-N≡N group. The signal confirms the formation of 3-azidopropyltrimethoxysilane. Other absorption bands are 2843-2944 cm⁻¹ (C-H stretching from aliphatic -CH₂) and 1087 cm⁻¹ (Si-O). The FT-IR spectrum (Figure 1b) of N₃PTMS-g-Fe₃O₄ formed by grafting of Fe₃O₄ to 3-azidopropyltrimethoxysilane shows the characteristic band at 586 cm⁻¹ (Fe-O which indicates the bonding of Fe₃O₄) and 3435 cm⁻¹ (O-H stretch from Fe₃O₄ particle surface). 2923 and 2099 cm⁻¹ bands are for aliphatic C-H and -N-N≡N stretching vibrations respectively. The product carrying Fe₃O₄ undergoes click reaction with propargyl alcohol (Scheme 1). The FT-IR spectrum (Figure 1c) shows the bands formed from the product of click reaction. 1598 and 1467 cm⁻¹ represent absorption bands respectively for C=C and C-N stretching vibrations from the 1,2,3-triazole ring.

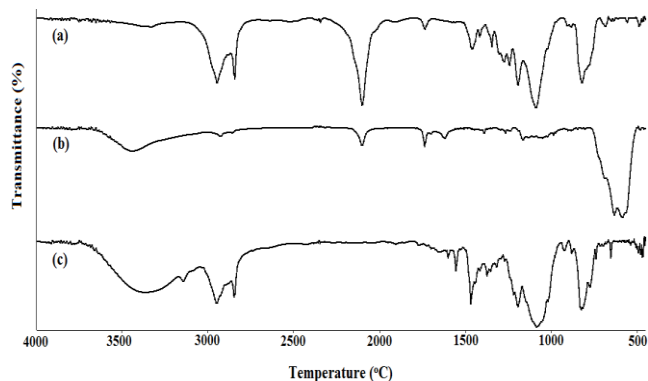
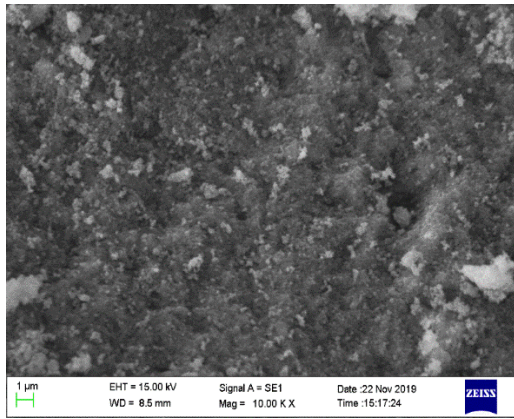
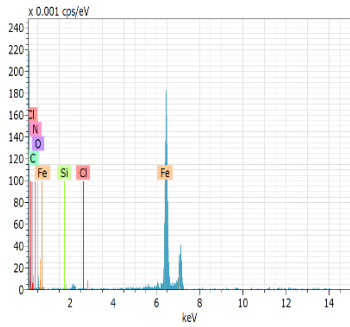


Figure 1. FT-IR spectra of (a) N₃PTMS (b) N₃PTMS-g-Fe₃O₄ and (c) POH-g-N₃PTMS-g-Fe₃O₄

Figure 2a and Figure 3a depict (SEM) images of N₃PTMS-g-Fe₃O₄ and POH-N₃PTMS-g-Fe₃O₄ respectively. The surface morphology of the modified magnetic nanoparticle and composites was examined at 10,000 magnification. It can be deduced that the Fe₃O₄ magnetic nanoparticle (Figure 2a) dominate in the sample and shows good uniformity. After click reaction with propargyl alcohol, the cubic structure of Fe₃O₄ magnetic nanoparticle (Figure 3a) becomes more prominent due to the formation of the 1,2,3-triazole ring. The compositional ratio and the type of constituents was determined using the EDX analysis for the samples shown in Figure 2b and 3b. Fe, C, O, N, Si, and Cl are present in both the samples with different percentages. SEM images of 5 and 20% POH-N₃PTMS-g-Fe₃O₄/PVC composite are respectively depicted in Figures 4a and Figure 5a. The composite showed that most of the POH-N₃PTMS-g-Fe₃O₄ are dispersed well within the PVC matrix with good uniformity and minor irregularities that are more visible on a 20% composite image at the lower part of the sample which is probably due to higher concentration of POH-N₃PTMS-g-Fe₃O₄ in the composite. EDX image in Figures 4b and Figure 5b reveal the presence of Fe, C, Cl, O, N, and Si in both composite samples.

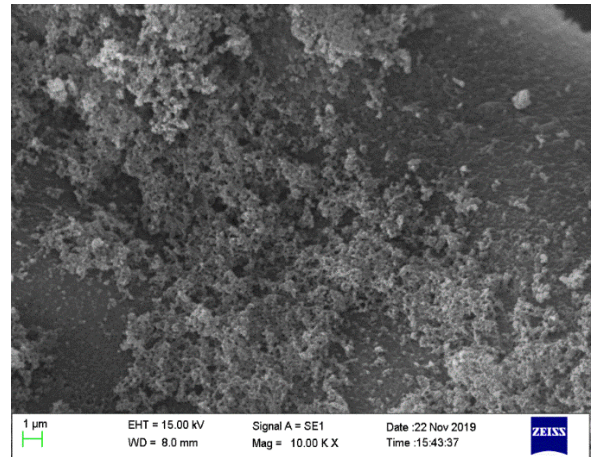


(a)

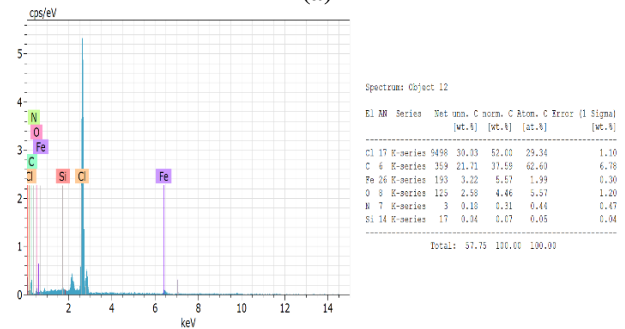


(b)

Figure 2. (a) SEM and (b) EDX images of N₃PTMS-g-Fe₃O₄

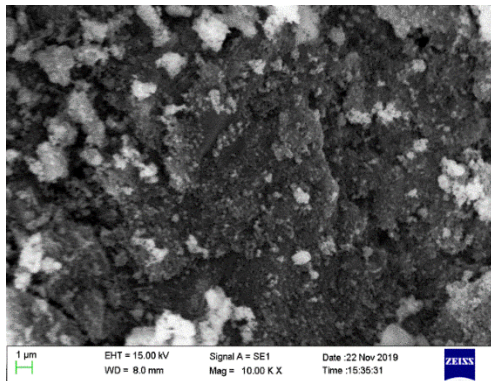


(a)

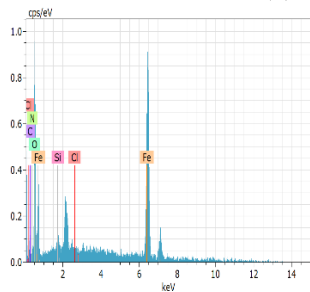


(b)

Figure 4. (a) SEM and (b) EDX images of PVC / 5% POH-N₃PTMS-g-Fe₃O₄ composite

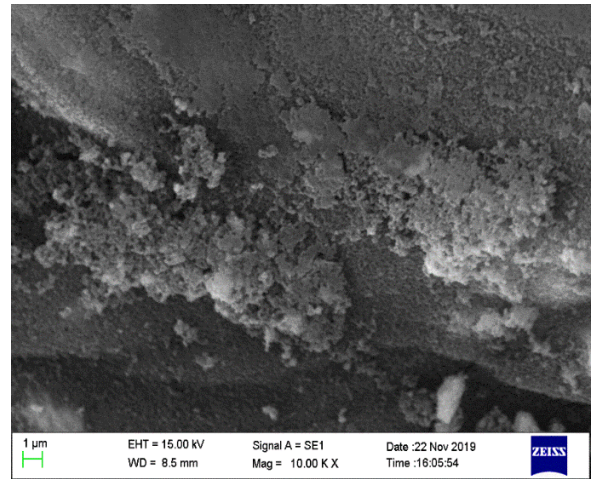


(a)

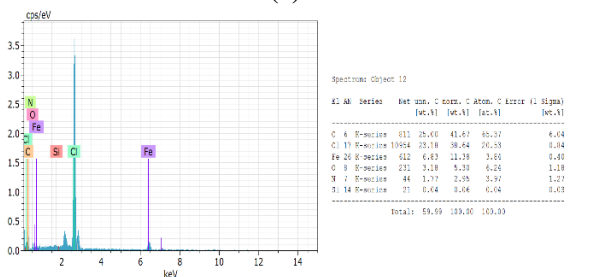


(b)

Figure 3. (a) SEM and (b) EDX images of POH-g-N₃PTMS-g-Fe₃O₄



(a)



(b)

Figure 5. (a) SEM and (b) EDX images of PVC / 20% POH-N₃PTMS-g-Fe₃O₄ composite

3.2. Magnetic investigation

The magnetic property of PVC/10% POH-N₃TMS-g-Fe₃O₄ composite was studied using a vibrating sample magnetometer (VSM) at 300K. From Figure 6, it can be seen that the magnetization curve has s-shaped over the applied magnetic field and the sample, 10% PVC-g-POH-N₃TMS-g-Fe₃O₄ composite showed saturation magnetization (M_s) around 5.12 emu/g which is far lower than M_s values of pure Fe₃O₄ nanoparticle reported in literature. The Fe₃O₄ nanoparticle bonded to PVC with the help of click reaction showed M_s of 41.5 emu/g [11]. The M_s value from the VSM plot is essential evidence of the presence of Fe₃O₄ magnetic nanoparticles within the composite.

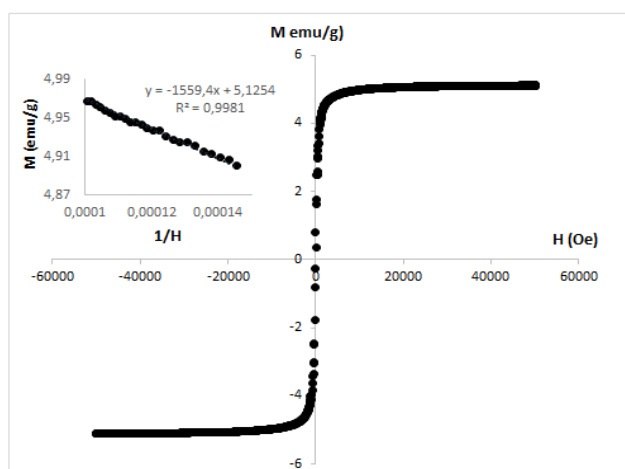


Figure 6. VSM plot of 10% PVC / POH-g-N₃PTMS-g-Fe₃O₄ composite

3.3. Thermal investigation

DSC curves of N₃PTMS-g-Fe₃O₄ and POH-N₃PTMS-g-Fe₃O₄ are depicted in Figure 7. The glass transition temperatures (T_g) determined based on the intermediate of the glass transition region and listed in Table 1. The T_g of 61 °C was recorded before click reaction with propargyl alcohol and the T_g of 57 °C was recorded after click reaction. The T_g was decreased by increasing the chain flexibility of the POH-N₃PTMS-g-Fe₃O₄ as a result of click reaction. TGA curves of N₃PTMS-g-Fe₃O₄ and POH-N₃PTMS-g-Fe₃O₄ are depicted in Figure 8. The initial decomposition temperatures (T_i) of N₃PTMS-g-Fe₃O₄ and POH-N₃PTMS-g-Fe₃O₄ are respectively 226 and 217 °C. The decrease in thermal stability of POH-N₃PTMS-g-Fe₃O₄ related to N₃PTMS-g-Fe₃O₄ is attributed to the formation of the 1,2,3-triazole ring. It can be observed that at 400 °C, the % mass loss of N₃PTMS-g-Fe₃O₄ is 4.6% which is lower than 7.0% for POH-N₃PTMS-g-Fe₃O₄. The friction of mass loss inconsistent also with the formation of the triazole ring through click

reaction. For different temperature readings, the percentage can also be determined. For instance, the residues percent at 800 °C are recorded as 92.4 and 88.5, respectively. The reason for the higher mass loss (%) at 400 °C and a lower % residue at 800 °C for POH-N₃PTMS-g-Fe₃O₄ is probably the click reaction. This is because click reaction increases the linearity of the POH-N₃PTMS-g-Fe₃O₄ which increases the free volume (decrease in T_g). The increase in free volume makes the POH-N₃PTMS-g-Fe₃O₄ susceptible to rapid % mass loss at 400 °C.

Figure 9 depicts the DSC curves of 5, 10, and 20% PVC-g-POH-N₃PTMS-g-Fe₃O₄ composites. When the amount of PVC increased from 5% to 10%, the T_g value increased from 60 to 72 °C. This is because when the PVC percentage is used more than 5%, the distance between the chains does not change much, i.e., when the ratio is exceeded 10%, the distance between the chains decreases, and hence, decreases the free volume in the polymer. The T_g value for 20% composite is 73 °C which was very close to that of 10% composite even though the 20% composite has POH-N₃PTMS-g-Fe₃O₄ contents as twice as the composite contains 10% PVC. In other words, the POH-N₃PTMS-g-Fe₃O₄ added has not considerably affected their T_g temperatures. A worth mentioning outcome from Table 2 is the increase in the T_g temperature of the composites as the POH-N₃PTMS-g-Fe₃O₄ percentage increases in each composite. This result implies that the presence of POH-N₃PTMS-g-Fe₃O₄ within the PVC matrix decreases the free volume of the composite which leads to an increase in the glass transition temperature (T_g) of the composite. TGA curves of 5, 10, and 20% PVC/POH-N₃PTMS-g-Fe₃O₄ composites are shown in Figure 10. The initial decomposition temperatures (T_i) of 5, 10, and 20 % composites are respectively 203, 210, and 217 °C. It can be seen that there is an increase in the thermal stability of the composites due to the increase in POH-N₃PTMS-g-Fe₃O₄ contents within the PVC matrix which is in line with the T_g observed from the DSC curves. Also, the TGA curve at 300 °C shows that the % mass loss is 57 for the 5% composite. The % mass loss increases to 79 for the 10% composite, while this value for 20% composite reaches 44. This implies that the rate of thermal decomposition of the composites is independent of the percentages of POH-N₃PTMS-g-Fe₃O₄ used in the composite preparation. For composites containing 5%, 10%, and 20% PVC, the residue at 450 °C were observed to be 3.2, 7.7, and 11.4, respectively. The observed residue is obviously as a result of the high amount of POH-N₃PTMS-g-Fe₃O₄ in the 20 % composite compared to 5% and 10% composites.

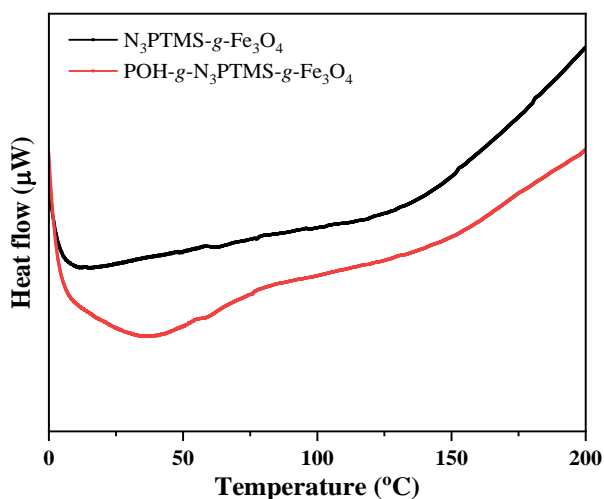


Figure 7. DSC curves of $N_3PTMS-g-Fe_3O_4$ and $POH-g-N_3PTMS-g-Fe_3O_4$

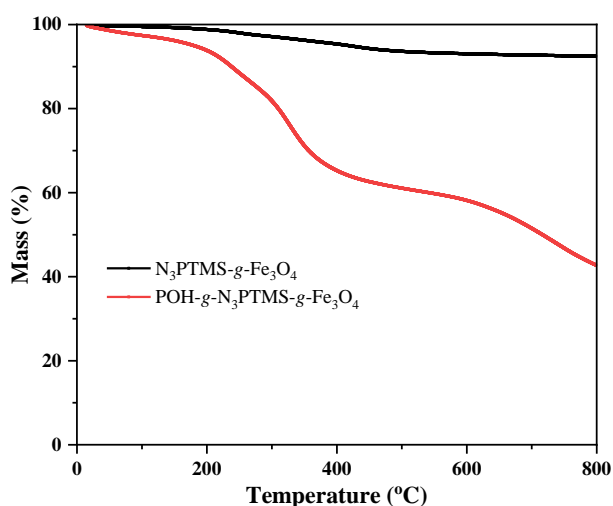


Figure 8. TGA curves of $N_3PTMS-g-Fe_3O_4$ and $POH-g-N_3PTMS-g-Fe_3O_4$

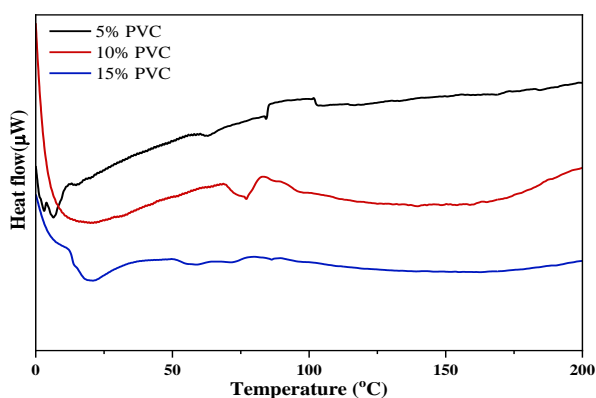


Figure 9. DSC curves of composites containing 5% PVC, 10% PVC, and 20% PVC

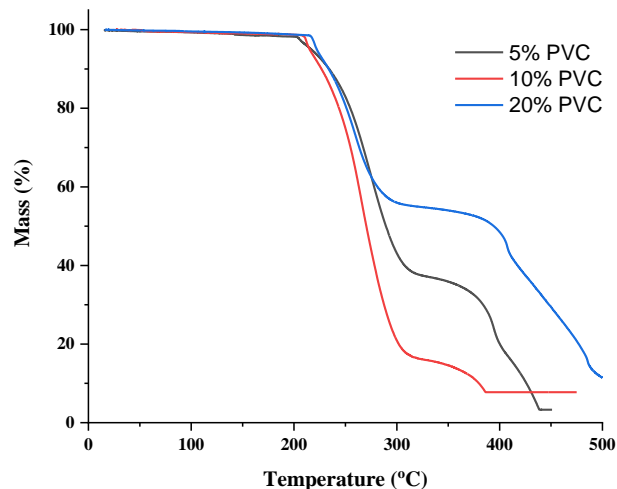


Figure 10. TGA curves of 5%, 10% and 20% $PVC-g-POH-N_3PTMS-g-Fe_3O_4$ composites

Table 1. Thermal investigation of modified Fe_3O_4

Modified Fe_3O_4	T_g (°C)	T_i (°C)	% Mass Loss at 400 °C	% Residue at 800 °C
$N_3PTMS-g-Fe_3O_4$	61	226	4.6	92.4
$POH-g-N_3PTMS-g-Fe_3O_4$	57	217	35.0	43

Table 2. Thermal investigation of $PVC-g-POH-g-N_3PTMS-g-Fe_3O_4$ composites

Composites	T_g (°C)	T_i (°C)	% Mass Loss at 300 °C	% Residue at 450 °C
5% composite	60	203	57	3.2
10% composite	72	210	79	7.7
20% composite	73	217	44	28

3.4. Electrical investigation

The concept of permeability, which is the ratio of dielectric permeability to vacuum permeability, refers to the ability of a material to be polarized. In order for the dielectric constant to be great, the polarization developed by the material in an applied field must be great. Some times, polar polymers need to align the dipoles. At very high frequencies, the dipoles do not have enough time to align before the field direction changes, but at low frequencies they have sufficient time. In the intermediate frequencies, although the dipoles move, they have completed their movements before the field direction changes [11]. Impedance analyzer is a well-known technique used for

characterizing the dielectric properties of the POH-N₃PTMS-g-Fe₃O₄ and its 5, 10, and 20% composites. The dielectric constant (ϵ'), dielectric loss (ϵ'') and AC conductivity (σ_{ac}) are used to characterize the electrical response of a polymer, copolymer, and composite material. They were measured within the same frequency range at room temperature except for the ϵ'' of the composites. Even though mobilization of the dipoles rests on the softness of a material, the dipoles in a polymeric material display a trend to orient in the direction of an applied field [17]. For POH-N₃PTMS-g-Fe₃O₄, ϵ' , ϵ'' , and σ_{ac} are depicted in Figure 11. The variation of dielectric constant (ϵ') with frequency at room temperature is almost the same as that of dielectric loss (ϵ''). At higher frequency, a rapid decrease was observed to a frequency of around 900 Hz, very slowly to a frequency of 5000 Hz, and then continue more or less constant. For the AC conductivity (σ_{ac}) at a higher frequency, it increased rapidly to a frequency of 900 Hz, the increment becomes very slow up to an approximate frequency of 5000 Hz and then continuous more or less linearly with an increase in applied frequency. The inset graphs in Figure 12a depicts the variation of ϵ' of composites with frequency at room temperature. From the graph, it was observed that the ϵ' of the composites increases with increasing POH-N₃PTMS-g-Fe₃O₄. The ϵ' values of 5, 10, and 20% composites are 2.2, 3.0, and 3.9 respectively compared to that of pure POH-N₃PTMS-g-Fe₃O₄ which is 6.0. The main cause in this increase in composites ϵ' seems to be the sequential addition of POH-N₃PTMS-g-Fe₃O₄ into the composite. In this context, effective interaction depends on enhancing the compatibility between POH-N₃PTMS-g-Fe₃O₄ and the PVC matrix through dispersion process which reduces the cohesive forces in the PVC chain leading to an increase in segmental mobility in the composite and hence, more dipoles are developed. The variation of dielectric loss of the composites (Figure 12b) shows an anomalous behavior as the applied frequency is increased at room temperature. Figure 12c demonstrates the variation of σ_{ac} in composites as a function of frequency. The σ_{ac} increases with increasing the applied frequency. Its also observed that the conductivity of the composite increases with an increase in the amount of POH-g-N₃PTMS-g-Fe₃O₄ within the composite.

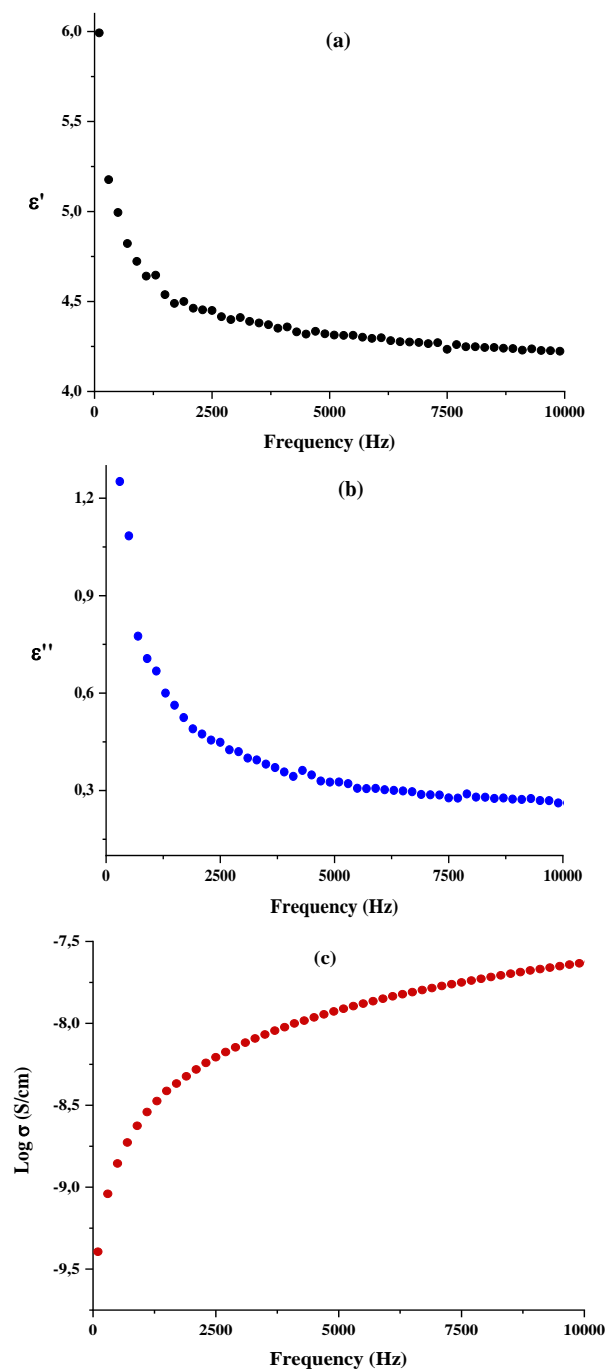


Figure 11. Variation of (a) dielectric constant (b) dielectric loss and (c) AC conductivity of POH-N₃PTMS-g-Fe₃O₄ with frequency at room temperature.

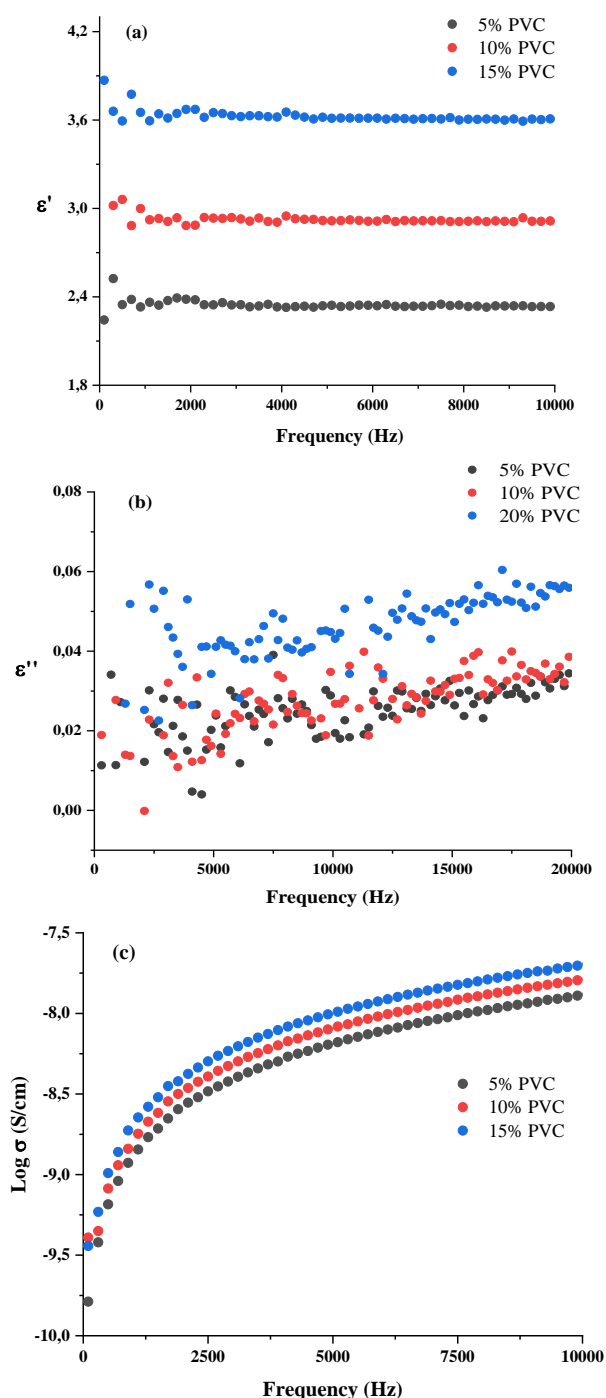


Figure 12. Variation of (a) dielectric constant (b) dielectric loss and (c) AC conductivity of PVC/POH-N₃PTMS-g-Fe₃O₄ composites with frequency at room temperature.

4. Conclusions

The effect on the structure, thermal, and dielectric properties of POH-N₃PTMS-g-Fe₃O₄ obtained by click reaction on 5, 10, and 20% PVC composites were investigated. FT-IR spectroscopy and SEM-EDX techniques were used in the characterization process. The saturation magnetization value (M_s) of the composite was calculated as 5.12 emu/g from the magnetization curve. Thermal analysis of N₃PTMS-g-

Fe₃O₄, POH-N₃PTMS-g-Fe₃O₄, and the PVC/POH-N₃PTMS-g-Fe₃O₄ composites were carried out to investigate the influence of the amount POH-N₃PTMS-g-Fe₃O₄ on the thermal behavior of the composites. It was observed that the glass transition temperature (T_g) value of N₃PTMS-g-Fe₃O₄ is higher than that of POH-N₃PTMS-g-Fe₃O₄ due to the formation of the 1,2,3-triazole ring. Likewise, the T_g of the composites increases as the amount of POH-N₃PTMS-g-Fe₃O₄ is increased. The result implies that the presence of POH-N₃PTMS-g-Fe₃O₄ within the PVC matrix decreases the free volume, and thus, the T_g of the composites increases. Initial decomposition temperature (T_i) was found to be 226 °C and 217 °C for N₃PTMS-g-Fe₃O₄ and POH-N₃PTMS-g-Fe₃O₄ respectively. For the composites, it was observed that the thermal stability of the composites increases with increasing the friction of POH-N₃PTMS-g-Fe₃O₄. Initial decomposition temperature (T_i) were 203 °C for 5%, 210 °C for 10%, and 217 °C for 20% PVC-g-POH-N₃PTMS-g-Fe₃O₄ composites. An increase in the thermal stability of the composites was due to the increase in the amount of POH-N₃PTMS-g-Fe₃O₄ within the PVC matrix, and hence, it conform the T_g results observed from the DSC curves. Also, the residue of N₃PTMS-g-Fe₃O₄ was 92.4% in Table 1, while the residue of POH-N₃PTMS-g-Fe₃O₄ due to the decomposition of both N₃PTMS and POH organic groups in the structure was found to be 43%. The dielectric constant (ϵ') and dielectric loss factor (ϵ'') for POH-N₃PTMS-g-Fe₃O₄ decreased with an increase in applied frequency and for the AC conductivity (σ), it increased rapidly with an increase in applied frequency. For the composites prepared, it was observed that the dielectric constant, dielectric loss factor, and AC conductivity increased as the POH-N₃PTMS-g-Fe₃O₄ percentage increased within the PVC matrix. The ϵ' values of 5, 10, and 20% composites were 2.2, 3.0, and 3.9 respectively.

Acknowledgment

The authors would like to thank the Firat University Scientific Research Projects Coordination Unit (FÜBAP) for the financial support of this research, Elazığ, Turkey, project number FF.18.18.

Conflicts of interest

The authors state that did not have conflict of interests

References

- [1] Wilson J., Poddar P., Frey N., Srikanth H., Mohamed K., Harmon J., Kotha S. and Wachsmuth J. Synthesis and magnetic properties of polymer nanocomposites with embedded iron

- nanoparticles. *Journal of Applied Physics*, 95 (2004) 1439-1443.
- [2] Frounchi M., Hadi M. Effect of synthesis method on magnetic and thermal properties of polyvinylidene fluoride/Fe₃O₄ nanocomposites. *Journal of Reinforced Plastics and Composites*, 32 (2013) 1044-1051.
- [3] Omid M. H., Alibeygi M., Piri F. and Masoudifarid M. Polystyrene/magnetite nanocomposite synthesis and characterization: investigation of magnetic and electrical properties for using as microelectromechanical systems (MEMS). *Materials Science-Poland*, 35 (2017) 105-110.
- [4] Chávez-Guajardo A. E., Medina-Llamas J. C., Maqueira L., Andrade C. A., Alves K. G. and de Melo C. P. Efficient removal of Cr (VI) and Cu (II) ions from aqueous media by use of polypyrrole/maghemite and polyaniline/maghemite magnetic nanocomposites. *Chemical Engineering Journal*, 281 (2015) 826-836.
- [5] Haruna H., Pekdemir M. E., Tukur A. and Coşkun M. Characterization, thermal and electrical properties of aminated PVC/oxidized MWCNT composites doped with nanographite. *Journal of Thermal Analysis and Calorimetry*, (2020) 1-9.
- [6] Qiu F., He G., Hao M. and Zhang G. Enhancing the Mechanical and Electrical Properties of Poly (Vinyl Chloride)-Based Conductive Nanocomposites by Zinc Oxide Nanorods. *Materials*, 11 (2018) 2139.
- [7] Tao Y., Feng W., Ding G. and Cheng G. Polyaniline nanorods/PVC composites with antistatic properties. *Russian Journal of Physical Chemistry A*, 89 (2015) 1445-1448.
- [8] Habashy M. M., Abd-Elhady A. M., Elsad R. and Izzularab M. A. Performance of PVC/SiO₂ nanocomposites under thermal ageing. *Applied Nanoscience*, (2019) 1-9.
- [9] Yazdani H., Hatami K., Khosravi E., Harper K. and Grady B. P. Strain-sensitive conductivity of carbon black-filled PVC composites subjected to cyclic loading. *Carbon*, 79 (2014) 393-405.
- [10] Yao K., Gong J., Tian N., Lin Y., Wen X., Jiang Z., Na H. and Tang T. Flammability properties and electromagnetic interference shielding of PVC/graphene composites containing Fe₃O₄ nanoparticles. *Rsc Advances*, 5 (2015) 31910-31919.
- [11] Tukur A., Pekdemir M. E., Haruna H. and Coşkun M. Magnetic nanoparticle bonding to PVC with the help of click reaction: characterization, thermal and electrical investigation. *Journal of Polymer Research*, 27 (2020) 161.
- [12] Ramesan M., Privya P., Jayakrishnan P., Kalaprasad G., Bahuleyan B. and Al-Maghrabi M. Influence of magnetite nanoparticles on electrical, magnetic and thermal properties of chitin/cashew gum biopolymer nanocomposites. *Polymer Composites*, 39 (2018) E540-E549.
- [13] Kirchberg S., Rudolph M., Ziegmann G. and Peuker U. Nanocomposites based on technical polymers and sterically functionalized soft magnetic magnetite nanoparticles: synthesis, processing, and characterization. *Journal of Nanomaterials*, 2012 (2012).
- [14] Namanga J., Foba J., Ndinteh D. T., Yufanyi D. M. and Krause R. W. M. Synthesis and magnetic properties of a superparamagnetic nanocomposite "pectin-magnetite nanocomposite". *Journal of Nanomaterials*, 2013 (2013).
- [15] Aliabadi M., Shagholani H. Synthesis of a novel biocompatible nanocomposite of graphene oxide and magnetic nanoparticles for drug delivery. *International journal of biological macromolecules*, 98 (2017) 287-291.
- [16] Singh R., Puri J. K., Sharma R. P., Malik A. K. and Ferretti V. Synthesis, characterization and structural aspects of 3-azidopropylsilatrane. *Journal of Molecular Structure*, 982 (2010) 107-112.
- [17] González-Guisasola C., Ribes-Greus A. Dielectric relaxations and conductivity of cross-linked PVA/SSA/GO composite membranes for fuel cells. *Polymer Testing*, 67 (2018) 55-67..